Macromolecular Chemistry and Physics
www.mcp-journal.de

# Radically Accessing D–A Type Ambipolar Copolymeric Materials with Intrinsic Electrical Conductivity and Visible–Near Infrared Absorption Via Electro-Copolymerization

*Tharindu A. Ranathunge, Dilan Karunathilaka, Duong T. Ngo, Nuwan H. Attanayake, Phillip Brodgon, Jared H. Delcamp, R. M. Gamini Rajapakse,* and Davita L. Watkins**

**Thienothiadiazole-bisthiophene ($TTDT_2$) and diketopyrrolo–pyrrole–bisthiophene ($DPPT_2$) are successfully electro-copolymerized with terthiophene ($T_3$) as an initiator and linker at low oxidative potentials. AC impedance analysis, absorption spectroscopy, and elemental composition via SEM-EDX support the formation of donor–acceptor (D–A) type alternating block copolymers, poly($T_3$-$TTDT_2$), and poly($T_3$-$DPPT_2$). Unique optical properties that span into the near infrared-II(>1000 nm) region and inherent electrical conductivity at the p-type regime, n-type regime, and in between the two regimes (i.e., typical insulator region) are observed. This study showcases the advantages of electro-polymerization toward tailoring of next generation opto-electronic materials.**

## 1. Introduction

Research in near infrared-II or NIR-II (1000–1700 nm) absorbing and emitting materials has risen as scientists have begun to take advantage of the innate properties of the spectrum for light harvesting and imaging.[1,2] Recent progress has demonstrated the effectiveness of adapting a donor–acceptor (D–A) motif to access the second NIR window and fine tune physical and optical properties.[3,4] Such works have revealed systematic band gap engineering of D–A material to achieve low energy transitions in electrically conducting polymers suitable for applications ranging from NIR-modulated cancer chemotherapy to organic solar cells.[5–8] However, challenges in structural engineering and synthesis have hindered the accessibility of these materials.[7,9,10]

Recently, we documented the preparation of NIR fluorescent thienothiadizole (TTD) dyes with large Stokes shifts (>161 nm) and high fluorescent quantum yields (>16%).[11] These molecules demonstrated optical absorption onsets ($\lambda_{onset}^{abs}$) in the NIR region between 730 and 850 nm and emission onsets ($\lambda_{onset}^{em}$) falling within 950–1000 nm. Notably, an increase in the number of thiophene units at both sides of TTD resulted in improved NIR-II optical properties with shifts toward longer wavelengths. However, the poor yields obtained in successive synthetic steps hampered further investigation. In this work, we take advantage of the distinctive properties of thienothiadiazole-bisthiophene ($TTDT_2$) via electro-copolymerization with terthiophene ($T_3$) to afford an alternating block copolymer, poly($T_3$-$TTDT_2$) (**Figure 1**). We compared the material to a diketopyrrolo–pyrrole–bisthiophene ($DPPT_2$)-based copolymer, poly($T_3$-$DPPT_2$), and a conventional homopolymer, polythiophene (poly$T_3$).

Although conjugated polymers composed of $TTDT_2$ and $DPPT_2$ are well documented, these studies consist of lengthy chemical synthetic methods with moderate to low yields.[12–15] In this work, electropolymerization is used as a versatile "green approach" to synthesize complex organic conjugated polymers. We and others have reported on the application of electropolymerization as a low-cost and straightforward alternative strategy to chemical synthesis.[16–20] The synthesis of conjugated polymers can be conducted under mild conditions with direct deposition of polymers onto conducting substrates for further device fabrication which reduces contaminants that can alter electrical properties.[21–23] By utilizing electrochemical methods, polymerization sequences can be varied by changing the type and surface of the electrode as well as the concentration of each monomer.[24,25] The latter has been demonstrated in our previous work where we were able to successfully show copolymerization of benzothiadiazole (BTD)-based copolymers with controlled stoichiometric ratios.[19]

For this study, DPP was selected as a D–A control material for comparison to TTD. Polymers containing DPP as the acceptor have been shown to possess intriguing electrical properties and favorable results in electronic devices.[26,27]

T. A. Ranathunge, D. Karunathilaka, D. T. Ngo, P. Brodgon,
Prof. J. H. Delcamp, Prof. R. M. G. Rajapakse, Prof. D. L. Watkins
Department of Chemistry and Biochemistry
University of Mississippi
University, MS 38677, USA
E-mail: rmgr@pdn.ac.lk; dwatkins@olemiss.edu
N. H. Attanayake
Department of Chemistry
Temple University
Philadelphia, PA 19122, USA
Prof. R. M. G. Rajapakse
Department of Chemistry
University of Peradeniya
Peradeniya 20400, Sri Lanka
The ORCID identification number(s) for the author(s) of this article can be found under https://doi.org/10.1002/macp.201900289.

**DOI: 10.1002/macp.201900289**

 

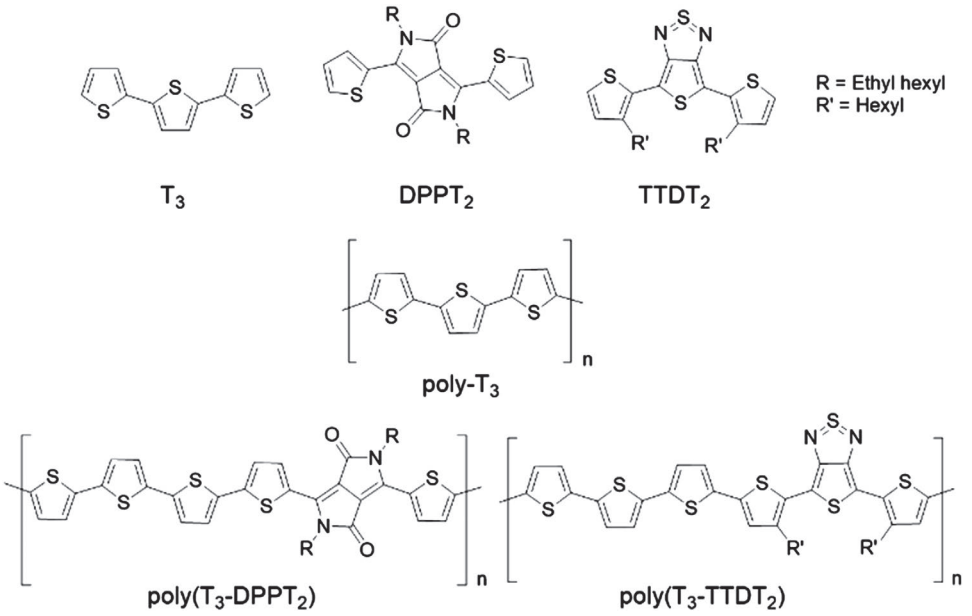


**Figure 1.** Structures of $T_3$, $TTDT_2$, and $DPPT_2$ monomers (top) and anticipated poly($T_3$-$TTDT_2$) and poly($T_3$-$DPPT_2$) copolymers (bottom) with conventional polythiophene (poly($T_3$)) (middle). Additional synthetic information is given in the Supporting Information.

Recently, electropolymerization of $DPPT_2$ and diketopyrrolo–pyrrole–bisfuran ($DPPF_2$) was documented alongside a comparison of their electrical and optical properties.[28,29] However, drastic conditions such as a 50-cycle cyclic voltammetric (CV) electrosynthesis in the potential range between −2 and + 2 V versus ferrocene/ferrocenium (Fc/Fc+) were employed. Such high oxidative potentials were required for polymerization as the thiophene (T) and furan (F) moieties are significantly electron deficient when attached to the DPP core due to the strong electron withdrawing nature of the acceptor moiety. This limitation can be overcome by copolymerizing $DPPT_2$ or $TTDT_2$ with $T_3$ as both the linker and initiator for electropolymerization. Herein, we report the details of that electrosynthesis and characterization of the resulting polymers, poly($T_3$-$TTDT_2$) and poly($T_3$-$DPPT_2$). The distinct features of the polymers (poly($T_3$-$TTDT_2$), poly($T_3$-$DPPT_2$), and (poly($T_3$)) are highlighted through electrochemical (cyclic voltammetry and AC impedance) and optical spectroscopic measurements (visible and NIR absorption). Improved electrical and optical properties are reported for the copolymers relative to conventional polymers. This transformative study of conductive polymers provides an efficient strategy toward complex materials with innumerable possible applications.

## 2. Results and Discussion

**Figure 2**a,b show successive CVs for the formation of the two copolymers of $T_3$ with $TTDT_2$ and $DPPT_2$, respectively. The polymers were formed on the working electrode (WE) surface and were rinsed with acetone to remove small soluble organic impurities. CVs ran in an argon purged background electrolyte (BGE) solution without monomers are shown in Figure 2c,d. Corresponding CVs for poly($T_3$) are given in Figure S4, Supporting Information. The copolymerization was achieved in ten repetitive CVs from 0 to +1.2 V versus saturated calomel electrode (SCE) with a potential scan rate of 100 mV $s^{-1}$. Additional details of the electro-copolymerization for $TTDT_2$ or $DPPT_2$ with $T_3$ are given in the Supporting Information.

The three polymers exhibit different redox characteristics as evident from their CVs (Figure 2c,d and Figure S5, Supporting Information). The process of electropolymerization to yield poly($T_3$) is well established[30–32] and assist in ruling out the possibility of forming poly($T_3$) alone. Poly($T_3$) has two oxidation onsets: one appearing at +0.639 V which is due to the formation of a cation radical at each monomeric unit of the polymer (i.e., poly(T—T—$T^{\bullet+}$)); and the second at +0.972 V due to the formation of a dication radical (i.e., poly($^{\bullet+}$T—T—$T^{\bullet+}$)). As such, $T_3$ can be polymerized at any potential above the first oxidation onset. However, the rate of polymerization at potentials between the two onsets (e.g., +0.800 V) is much lower than that of the second oxidation onset. This is confirmed by the large currents observed when $T_3$ is polymerized at +1.20 V compared to currents at +0.800 V. This observation is easily understood since the dication radical is capable of affording successive monomer units attached at both thiophene units in $T_3$ whereas the monocation radical can only add a single monomer at a time. In addition, higher potentials increase the concentration of reactive radical species and provides more energy to surmount activation energy barriers associated with polymer formation.

Our attempts to grow homopolymers of $TTDT_2$ or $DPPT_2$ through repetitive CVs in the range from 0 to +1.2 V were unsuccessful and the currents in the successive CVs declined rather than increased. It is important to note that although both $TTDT_2$ and $DPPT_2$ are electroactive within the potential range −1.5 to +1.2 V, neither are able to electropolymerize on their own within this potential range. However, both monomers can be copolymerized with $T_3$ under mild conditions from 0 to

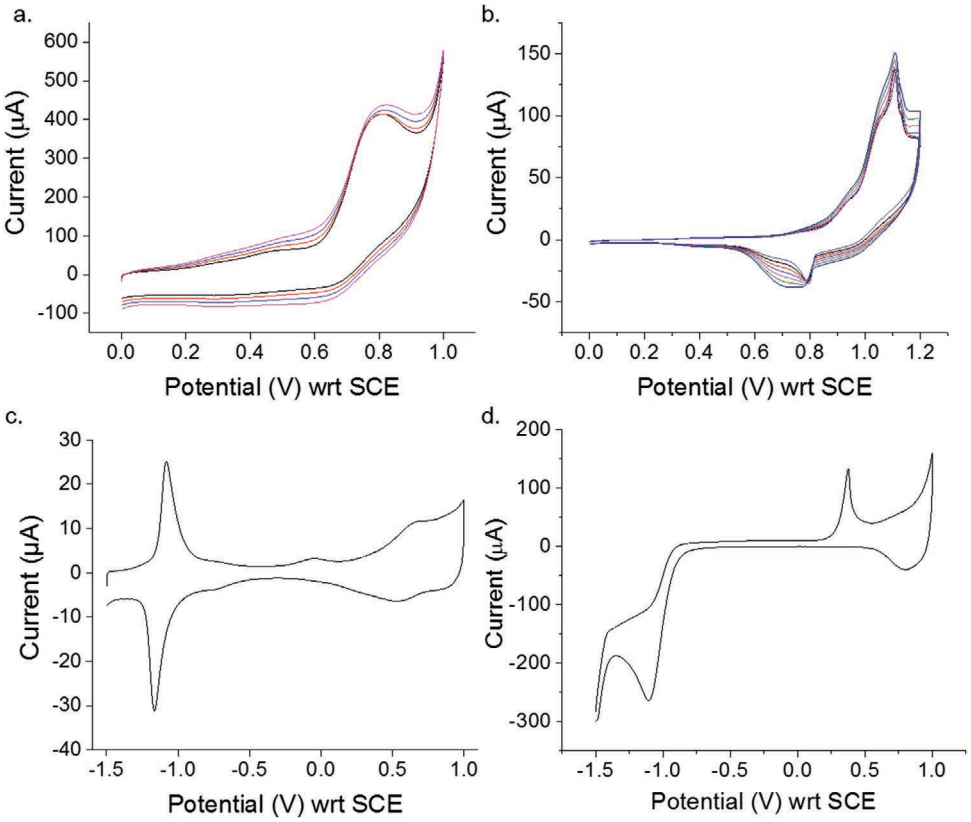


**Figure 2.** a,b) Repetitive CVs for the copolymerization of poly($T_3$-$TTDT_2$), poly($T_3$-$DPPT_2$). c,d) CVs of copolymers. CVs for poly($T_3$) are shown in the Supporting Information.

+1.2 V to result in corresponding copolymers as shown by the successive increase in currents in repetitive CVs and concomitant deposition of polymer films on the WE surfaces. These results provide evidence that $T_3$ is acting as both the polymerization initiator and linker between the two acceptor monomers, as without it these monomers are unable to form polymers.

Copolymer formation at potentials between the two oxidation potential onsets of $T_3$ are unfavorable when $T_3$ is copolymerized with $TTDT_2$ or $DPPT_2$. However, successful copolymerization was achieved, in both cases, when a potential above the second oxidation onset of $T_3$ was used. We speculate that $^{+\bullet}$T—T—T$^{\bullet+}$ is inducing the sequential oxidation of two thiophene units at both ends of the $TTDT_2$ or $DPPT_2$ monomers in the first propagation step to result in the formation of —T—TTD—T—$T_3$—T—TTD—T— and —T—DPP—T—$T_3$—T—DPP—T— units. These units then require $^{+\bullet}$T—T—T$^{\bullet+}$ for further propagation of the polymerization reaction. This would lead to the formation of alternating copolymers of $T_3$-$TTDT_2$ and $T_3$-$DPPT_2$ if only one $T_3$ is used to couple the other monomer units.

Additional insight into polymerization mechanism comes from the analysis of CVs of the polymers (Figure 2). Poly($T_3$) has a characteristic reduction peak potential ($E_p$) centered at +0.694 V (peak currents ($I_p$) = –27.33 μA, electric charge ($A_h$) = –17.39 μC) in the potential range from –1.5 to + 1.2 V (see Supporting Information). This peak in poly($T_3$-$TTDT_2$) and poly($T_3$-$DPPT_2$) has been shifted to +0.537 and +0.659 V, respectively. Neither of the corresponding acceptor monomers shows a reduction peak at or close to these potentials. The lowering of the $T_3$ reduction peak suggests that $T_3$ is bonded to more thiophene units in the copolymers such as when $T_5$ groups are formed during the synthesis of poly($T_3$-$DPPT_2$).

Evidence for the presence of $TTDT_2$ in the copolymer comes from respective redox peaks appearing in the negative potential range. The characteristic reduction peak at –1.165 V ($I_p$ = –22.50 μA, $A_h$ = –14.41 μC) and the return sweep oxidation peak at –1.081 V ($I_p$ = 22.17 μA, $A_h$ = 10.30 μC) (Figure 2c) can be assigned to be the redox behavior of TTD in the copolymers since $TTDT_2$ monomer (Figure S6, Supporting Information) shows redox peaks at potentials close to these values but poly($T_3$) does not (FigureS5, Supporting Information). The corresponding reduction peak for DPP in poly($T_3$-$DPPT_2$) is located at –1.103 V ($I_p$ = –26.35 μA) (Figure 2d and Figure S7, Supporting Information). The reduced form of DPP appears more stable than the reduced form of TTD since the corresponding oxidation peak of the former appears at a much higher potential of +0.375 V ($I_p$ = 9.86 μA). The reduction peaks for TTD or DPP in the copolymers have been shifted slightly negatively from those of the corresponding monomers suggesting that TTD or DPP units have become more difficult to reduce. Such an observation is common as the acceptor units draw electron density from the thiophenes present on either

**Table 1.** Electrical parameters extracted from Nyquist plots of AC impedance analyses of poly($T_3$-$TTDT_2$) and poly($T_3$-$DPPT_2$).

| Poly($T_3$-$TTDT_2$) | | | | | |
|---|---|---|---|---|---|
| DC potential [V] | $R_s$ [Ω] | $R_e$ [Ω] | $C_d$ [μF] | $W$ [μΩ] | $C$ [μF] |
| +0.8 | 130.4 | 82.36 | 0.018 | 119.6 | 34.53 |
| +0.7 | 158.5 | 88.24 | 0.056 | 814.8 | 32.56 |
| +0.6 | 105.8 | 89.45 | 0.074 | 691.1 | 24.51 |
| +0.4 | 170.6 | 91.50 | 0.096 | 602.2 | 15.78 |
| +0.2 | 168.0 | 94.78 | 0.246 | 657.4 | 7.688 |
| 0 | 92.27 | 1048 | 0.396 | 13.68 | 40.49 |
| −0.2 | 69.76 | 7699 | 0.121 | 12.16 | 1.245 |
| −0.4 | 64.09 | 9079 | 0.109 | 11.92 | 1.360 |
| −0.6 | 55.57 | 4285 | 0.173 | 10.64 | 4.948 |
| −0.8 | 136.7 | 1828 | 0.356 | 24.60 | 26.88 |
| −1.0 | 171.8 | 177.5 | 0.184 | 110.3 | 53.25 |
| −1.2 | 168.8 | 279.3 | 0.109 | 60.51 | 22.26 |
| −1.4 | 177.0 | 213.3 | 0.134 | 159.7 | 28.26 |
| Poly($T_3$-$DPPT_2$) | | | | | |
| DC potential [V] | $R_s$ [Ω] | $R_e$ [Ω] | $C_d$ [μF] | $W$ [μΩ] | $C$ [μF] |
| +1.2 | 59.41 | 176.3 | 1.662 | 2165 | 134.3 |
| +1.1 | 58.54 | 179.6 | 1.609 | 1482 | 110.6 |
| +1.0 | 55.42 | 185.1 | 1.499 | 1197 | 70.63 |
| +0.8 | 42.88 | 191.1 | 1.270 | 335.7 | 25.21 |
| +0.6 | 59.52 | 181.0 | 1.525 | 186.7 | 6.149 |
| +0.4 | 45.99 | 179.2 | 1.266 | 55.51 | 2.068 |
| +0.2 | 44.56 | 171.0 | 1.536 | 63.39 | 1.432 |
| +0.1 | 46.35 | 176.3 | 1.682 | 61.45 | 1.447 |
| −0.2 | 49.22 | 159.9 | 1.834 | 56.93 | 1.495 |
| −0.4 | 46.94 | 164.2 | 1.730 | 54.06 | 1.633 |
| −0.6 | 48.58 | 156.5 | 1.878 | 51.37 | 1.639 |
| −0.8 | 49.57 | 150.6 | 1.990 | 47.63 | 1.696 |
| −1.0 | 50.54 | 145.1 | 2.137 | 43.68 | 1.836 |
| −1.2 | 46.01 | 139.1 | 2.106 | 32.94 | 265.8 |
| −1.4 | 52.79 | 139.2 | 2.447 | 35.03 | 39.90 |

sides.[11] In poly($T_3$-$TTDT_2$) and poly($T_3$-$DPPT_2$), the acceptor core has become more electron rich yielding additional indirect evidence of copolymerization. The trends in current and charge values for redox peaks indicate that the two monomer units are most likely 1:1 and that poly($T_3$-$TTDT_2$) and poly($T_3$-$DPPT_2$) exhibit intriguing electrical properties.

Both copolymers show appreciable currents in the range from −1.5 to +1.2 V versus SCE via CV; therefore, electrical conductivities are expected at all measurable potentials within this range. AC impedance analysis was used to assess these electrical properties. Representative Nyquist plots of poly($T_3$-$TTDT_2$), poly($T_3$-$DPPT_2$), and poly($T_3$) together with the equivalent circuit used to analyze them are given in Figures S8–S14, Supporting Information. **Table 1** tabulates the electrical parameters which were extracted from fitting the experimental plots to theoretical ones generated from the equivalent circuit used (Table S1, Supporting Information). A dual rail transmission line circuit and a simplified equivalent circuit used for data extraction are also shown in the Supporting Information. The series resistance of the cell ($R_s$), resistance for electron transport along the polymer backbone ($R_e$), double layer capacitance between polymer–electrolyte interface ($C_d$), Warburg impedance for ingress and egress of counter ions by diffusion ($W$), capacitance of the high frequency pure capacitive regime ($C$) are also provided.

Typical of many conducting polymers, poly($T_3$) shows appreciable $R_e$ values only in the p-type (i.e., positive or cationic domain, oxidation) regime in the range from 100 to 200 Ω. Below +0.4 V, the polymer shows over 1 MΩ $R_e$ values down to about −1.2 V before n-type conducting behavior with $R_e$ values in the kΩ range is observed. Poly($T_3$-$TTDT_2$) is highly electronically conducting in the p-type regime above +0.2 V versus SCE with $R_e$ values less than 100 Ω which increase slightly as the applied positive potential is increased. The n-type (i.e., negative or anionic domain, reduction) regime below −1.0 V versus SCE has a one order of magnitude higher $R_e$ value than the p-type regime of the polymer indicative of electrical conductivity even in the n-type regime. The polymer has appreciable electronic conductivity between these two regimes where $R_e$ values are between 1 and 10 kΩ—an area where conventional electronically conductive polymers behave as insulators. The electrical conductivity data corroborates well with the trend in the CV of the polymer in the BGE where it shows high currents in the potential region between −1.5 to + 1.2 V with higher values at the ends. Interestingly, the $W$ which represents ion transport resistance by diffusion is much lower (10–25 μΩ) in potential regimes where the polymer has higher $R_e$ values. In the p-type regime, $W$ values are between 100 and 815 μΩ while in the n-type regime, values are between 60 and 200 μΩ. The trend shown by poly($T_3$-$DPPT_2$) is even more intriguing: $R_e$ values lie between 130 and 190 Ω throughout the entire potential region from −1.5 to + 1.2 V. The $R_e$ values of poly($T_3$-$DPPT_2$) in the p-type regime are twice as high as those of poly($T_3$-$TTDT_2$). However, the $R_e$ values in the p-type regime are significantly lower than the $R_e$ values at the "in between" (typically the insulator region) and n-type regimes for poly($T_3$-$TTDT_2$). The $W$ values are also lowest in the "in between" and n-type regimes ranging from 30 to 65 μΩ for poly($T_3$-$TTDT_2$). The $W$ values are observed to increase progressively in the p-type regime from 100 to just over 2000 μΩ. The fact that both copolymers have appreciably high electrical conductivity—even in the absence of applied DC potential bias—indicates an inherent electrical conductivity generated from the intrinsic charge carriers present in the polymers. These intrinsic charge carriers may have originated from an intramolecular charge separation from electron donating thiophene units and electron withdrawing TTD or DPP units present in the polymer backbones.

Due to the presence of at least four thiophene units at either sides of the TTD or DPP units, the repeat units of the polymers are highly polarized possessing conjugated $TDD^{\bullet-}$ or $DPP^{\bullet-}$ (negative) polarons and $T^{\bullet+}$ (positive) polarons in equal amounts in the intrinsic polymer. In poly($T_3$-$TTDT_2$), these charge carriers can be increased by one or two orders of magnitude by subjecting it to negative or positive potentials making it either an n- or p-type conductor. Observing increases in charge carriers of this magnitude is unique for ambipolar polymers

when compared with conventional electronically conducting polymers such as poly($T_3$).

Electrochemical analysis strongly suggest that poly($T_3$-$TTDT_2$) is an ambipolar polymer with an alternating diblock structure. Further support of polymer composition was done via SEM-EDX analysis. SEM images reveal the morphology of the polymers as films on FTO glass (see Supporting Information). Both poly($T_3$-$TTDT_2$) and poly($T_3$-$DPPT_2$) appear as agglomerated deposits over a more uniform polymer layer. Poly($T_3$-$DPPT_2$) shows an irregular pattern of amorphous aggregates. However, poly($T_3$-$TTDT_2$) exhibits a more flake-like morphology presumable due its more crystalline character relative to poly($T_3$-$DPPT_2$). Nonetheless, these morphologies—being either crystalline and amorphous—are deemed useful for further opto-electronic application.[33,34]

Polymer composition was confirmed via EDX analysis. Theoretically calculated atomic ratios for conceivable monomer arrangements (i.e., poly[$(T_3)_n$$DPPT_2$] or poly[$(T_3)_n$$TTDT_2$], where $n = 1, 2, 3, 4$) were considered and compared with experimental data (Table S2, Supporting Information). Notably, the atomic ratios obtained from SEM-EDX are complicated due to the interference from the atoms of FTO and the glass substrate. In both polymers, oxygen appears to a higher extent than theoretically calculated presumably due to the substrate contribution. In lieu of excess oxygen, carbon percentages appear somewhat lower. Although accurate determination of carbon and oxygen are quite difficult, sulfur and nitrogen content appear close to theoretical values calculated for the alternating copolymers where $n = 1$ for poly[$(T_3)_n$$TTDT_2$] and poly[$(T_3)_n$$DPPT_2$]. In turn, the results indicate that the experimental percentages match closely with the proposed alternating diblock structure. This is further supported by the fact that neither $TTDT_2$ nor $DPPT_2$ could be polymerized without $T_3$.

Driven toward possible practical application, the stability of the polymers were evaluated by subjecting the polymers to repeated redox cycles (4000 cycles) between +1.2 and −1.5 V (Figure S15, Supporting Information). The first and last cycles were compared to observe the redox stability of the polymer—specifically seeking any signs of electrochemical decay due to structural distortion and/or degradation.[35,36] For both poly($T_3$-$TTDT_2$) and poly($T_3$-$DPPT_2$), the total exchange charge remains constant for each cycle indicating that the redox activities remain the same even at 4000 cycles.[37] Interestingly, the current increases by ≈1 µA for poly($T_3$-$TTDT_2$) and 20 µA for poly($T_3$-$DPPT_2$). Such a phenomenon is indicative of highly stable D–A materials as more current is required to pass through them with increasing redox cycles at constant potential. In addition, no peak potential shifts were detected over these repeated cycles. These results indicate an electroactive and stable polymer applicable for numerous applications.[37–39]

Our strategy of electro-copolymerization of D–A type monomer units with more donor monomers as linkers has opened up a simple and one-step method to form ambipolar copolymers with intriguing electrical properties. The fact that these ambipolar polymers have high electronic conductivities indicate that they are true conductors rather than semiconductors. This means that both copolymers must have very low or negligible band gaps. Accordingly, all the polymers show optical absorption in the range from 400 to 1800 nm (**Figure 3** and Table S3, Supporting Information). Poly($T_3$) has three absorption maxima in its n-type state (i.e., negatively biased via voltammetry) in 600–800, 800–1200, and 1200–1800 nm ranges. The first two maxima are barely visible in the p-type state (i.e., positively biased via voltammetry) though the third maxima appears clearly in the absorption spectrum. However, the absorption values reach zero at 1800 nm in both forms. In poly($T_3$-$TTDT_2$), the first and third maxima are visible though almost no absorption is observed in the second region from 800 to 1200 nm region in both n- and p-type states. The absorption values do not reach zero even at 1800 nm indicating that the absorption onset is lying further into higher wavelengths of the NIR region beyond the spectrometer limits. In poly($T_3$-$DPPT_2$), the trend is again different showing little to no absorption in the first region but clearly showing maxima in the second and third regions with an onset penetrating above 1800 nm.

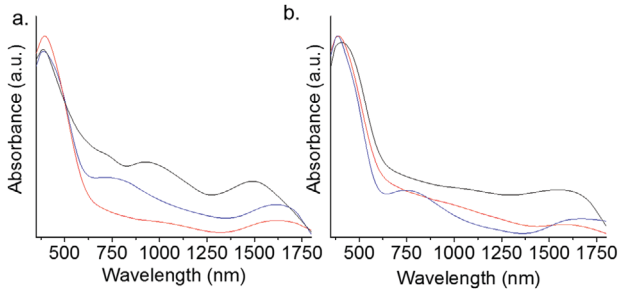


**Figure 3.** UV–visible–NIR spectra a) n-type and b) p-type; poly($T_3$)—black; poly($T_3$-$TTDT_2$)—blue, and poly($T_3$-$DPPT_2$)—red. Additional absorbance spectra of poly($T_3$) and energy level diagrams for poly($T_3$), poly($T_3$-$TTDT_2$), and poly($T_3$-$DPPT_2$) are in the Supporting Information.

The $\pi \rightarrow \pi^*$ transitions of conjugated electronically conducting polymers occur in the visible range where the energy gap is determined by the extent of conjugation (Table S3, Supporting Information). Conductivity data of poly($T_3$) suggest that when the p-type polymer is subjected to negative potentials down to −1.2 V, the polymer backbone becomes neutral rather than negatively charged making the polymer n-type. In this non-conducting state, poly($T_3$) has a $\lambda_{max}$ value corresponding to a $\pi \rightarrow \pi^*$ transition at 365 nm ($E_g^{opt}$ = 3.40 eV). Energy gaps for copolymers of poly($T_3$-$TTDT_2$) and poly($T_3$-$DPPT_2$) are 2.93 and 3.34 eV, respectively (Table S3, Supporting Information). In the p-type state, the corresponding band gaps are 3.32, 2.81, and 3.02 eV, respectively (Table S3, Supporting Information).

Although $\pi \rightarrow \pi^*$ transitions have large energy gaps, the polaron and bipolaron levels with considerable low energy gaps (Figures S17–S19, Supporting Information) yield materials with electrical conductivity comparable to metals in their doped states.[40,41] The polaron levels for poly($T_3$), poly($T_3$-$TTDT_2$), and poly($T_3$-$DPPT_2$) appear at $\lambda_{max}$ of 947 nm (1.72 eV), 741 nm (1.67 eV), and 990 nm (1.25 eV), respectively, for films subjected to negative potentials. Corresponding values in p-type state are 933 nm (1.25 eV), 745 nm (1.61 eV), and 1008 nm (1.23 eV), respectively. Bipolaron levels of negative poly($T_3$), poly($T_3$-$TTDT_2$), and poly($T_3$-$DPPT_2$) are located at 1497 nm (0.828 eV), 1624 nm (0.763 eV), and 1561 nm (0.828 eV), respectively. In the p-type state, they are located at 1580 nm (0.80 eV), 1671 nm (0.70 eV), and 1630 nm (0.76 eV), respectively. Electronic conductivity in the doped states are dominated by bipolaron

transitions involving less than 1 eV energy gaps. The bipolaron energy gaps of the two copolymers are significantly lower than that of poly($T_3$) again demonstrating high doping and consequently high conductivity of the copolymers.

## 3. Conclusion

This work demonstrated the use of simple electropolymerization to prepare tailor-made D–A type copolymers possessing inherent electrical conductivity at both p- and n-type regimes and in between the two regimes. Comparison of electrochemical data for the monomers to that of the polymers stand as indirect evidence of polymerization. Elemental composition via SEM-EDX support the formation of D–A type alternating block copolymers. Compared to a conventional electronically conducting polymer, copolymers show improved electrical properties and optical absorption toward the NIR-II region. These results lay the foundation for additional transformative studies in the electrosynthesis of multifaceted copolymers with potential applications in opto-electronics.

## 4. Experimental Section

Reagents and solvents were purchased from commercial sources and used without further purification unless otherwise specified. Preparation of the monomeric units primarily followed the literature-reported syntheses of similar derivatives. Additional synthetic details can be found in the Supporting Information.

*Electrosynthesis*: All electrochemical experiments including AC impedance analysis were carried out using CH Instruments CHI6109E Electrochemical Analyzer upgraded to include AC impedance analysis. FTO slides were purchased from Sigma and all other electrodes from CH Instruments: Electrodes used are Saturated Calomel Reference Electrode (SCE) CHI150, Glassy carbon (GC) Working Electrode CHI104, and Pt-wire Counter Electrode CHI115. SCE was rinsed thoroughly with distilled water, wiped with paper tissue. GC was polished using 0.05 micron alumina powder on CHI polishing pad. Pt-wire CE was cleaned with concentrated nitric acid and rinsed thoroughly with distilled water and air dried. $T_3$ homopolymer and $T_3$-$DPPT_2$ and $T_3$-$TTDT_2$ copolymers were synthesized from an acetonitrile solution (10 mL) containing $T_3$, $DPPT_2$, and/or $TTDT_2$ monomer at 1 mM concentration and 0.10 M tetrabutylammonium hexafluorophosphate BGE on GC or fluoride-doped tin oxide (FTO) working electrode surface. The electrochemical cell was composed of the above WE, Pt-wire counter electrode, and SCE. The solution was purged with high purity argon gas for 20 min prior to all electrochemical experiments which were subsequently carried out under argon blanket. Scan rate of 100 mV $s^{-1}$ was used and potentials were referred with respect to SCE unless otherwise stated. Electropolymerization was achieved via cyclic voltammetry in the potential range from 0 to +1.2 V in repetitive CVs. When the upper limit of the potential was reduced to +0.8 V or +1.0 V, polymer deposition on the WE was not observed and the currents in the successive CVs declined rather than increasing. As such, an upper limit of +1.2 V wrt SCE was always used in the electrosynthesis of all polymers.

*Electrochemical and Electrical Characterization*: The polymers were formed on the WE surfaces were rinsed with acetone to remove small soluble organic impurities and their CVs were run in an argon purged BGE solution without monomers at a scan rate of 100 mV $s^{-1}$. However, for the scan rate ($v$) dependence of peak current ($I_p$) studies 1, 4, 9, 16, 25, 36, 49, 64, 81, and 100 mV $s^{-1}$ scan rates were chosen since these numbers give perfect square roots for accurate construction of $I_p$ versus $v^{1/2}$ plots.

In order to assess electrical properties of the homopolymer and copolymers, AC impedance analysis was carried out in its AC impedance mode in a three-electrode configuration containing argon purged BGE. Nyquist and Bode plots were recorded at different potentials from −1.5 to + 1.2 V. Nyquist plots were analyzed by the simulation software which was provided with the instrument. In order to do so, the dual rail transmission line model put forward by Albery et al.[42,43] and further refined by Pickup et al.[44,45] were used. The dual rail transmission line circuit (middle) and simplified equivalent circuit (bottom) used to extract data are also shown in Supporting Information.

*Morphology and Composition*: SEM images were obtained with a FEG Quanta 450 FEG Electron Microscope, operated at an acceleration voltage of 5 kV. A low acceleration voltage of 5 keV was chosen since polymers usually undergo burning when highly energetic electrons are incident on them at high acceleration voltages of 10 or 20 keV normally used for robust inorganic materials. Energy dispersive X-ray spectra (EDX) were obtained with an X-MaxN 50 spectrometer (Oxford Instrument) mounted on the SEM.

*Absorbance Spectroscopy*: UV–vis–NIR spectra were measured with a Cary 5000 instrument; energy level schematic derived from peak maximum and onset of peaks observed in the absorbance spectra. The second onset used unless otherwise noted. The polymer was deposited via cyclic voltammetry (CV) in the positive potential range from 0 to + 1.2 V. The working electrode was replaced by FTO glass with dimensions of 1 cm × 5 cm × 0.25 cm ($w \times h \times d$). Each trial was maintained on a scan rate of 100 mV $s^{-1}$ with 50 repetitive cycles. The deposited polymer on FTO glass was carefully taken out of the solution and rinsed with acetone to remove the excess monomers. Two blank FTO plates were used to run the baseline correction for absorbance. The upper and lower limits on the Cary 5000 were set to 2000–200 nm and the scan rate adjusted to 800 nm $s^{-1}$. Polymer deposited on the FTO glass was used in the sample holder parallel to the incident laser beam detecting the thin layer. Each sample was carried out for three trials and average onsets were calculated.

## Supporting Information

Supporting Information is available from the Wiley Online Library or from the author.

## Acknowledgements

R.M.G.R. is a visiting scholar at the University of Mississippi and is on leave from the University of Peradeniya, Sri Lanka The authors appreciate financial support of this work from the National Science Foundation under Grant Number NSF OIA-1757220. The authors also thank Dr. Daniel Strongin, professor and chair at Temple University, for access to SEM-EDX.

## Conflict of Interest

The authors declare no conflict of interest.

## Keywords

conducting polymers, conjugated polymers, donor–acceptor, electrochemistry, electropolymerization

Received: July 1, 2019
Revised: September 6, 2019
Published online:

[1] F. Ding, Y. Zhan, X. Lu, Y. Sun, *Chem. Sci.* **2018**, *9*, 4370.
[2] S. He, J. Song, J. Qu, Z. Cheng, *Chem. Soc. Rev.* **2018**, *47*, 4258.
[3] J. Zeng, Z. Wan, H. Li, P. Liu, W. Deng, *Sol. Energy Mater. Sol. Cells* **2018**, *178*, 223.
[4] Q. Yang, Z. Ma, H. Wang, B. Zhou, S. Zhu, Y. Zhong, J. Wang, H. Wan, A. Antaris, R. Ma, X. Zhang, J. Yang, X. Zhang, H. Sun, W. Liu, Y. Liang, H. Dai, *Adv. Mater.* **2017**, *29*, 1605497.
[5] G. L. Gibson, T. M. McCormick, D. S. Seferos, *J. Am. Chem. Soc.* **2012**, *134*, 539.
[6] D.-D. Li, J.-X. Wang, Y. Ma, H.-S. Qian, D. Wang, L. Wang, G. Zhang, L. Qiu, Y.-C. Wang, X.-Z. Yang, *ACS Appl. Mater. Interfaces* **2016**, *8*, 19312.
[7] F. Feng, L. Kong, H. Du, J. Zhao, J. Zhang, *Polymers* **2018**, *10*, 427.
[8] R. S. Kularatne, H. D. Magurudeniya, P. Sista, M. C. Biewer, M. C. Stefan, *J. Polym. Sci., Part A: Polym. Chem.* **2013**, *51*, 743.
[9] L. Dou, Y. Liu, Z. Hong, G. Li, Y. Yang, *Chem. Rev.* **2015**, *115*, 12633.
[10] G. Hong, A. L. Antaris, H. Dai, *Nat. Biomed. Eng.* **2017**, *1*, 0010.
[11] Y. Zhang, S. A. Autry, L. E. McNamara, S. T. Nguyen, N. Le, P. Brogdon, D. L. Watkins, N. I. Hammer, J. H. Delcamp, *J. Org. Chem.* **2017**, *82*, 5597.
[12] Y. N. Luponosov, J. Min, D. A. Khanin, D. Baran, S. A. Pisarev, S. M. Peregudova, P. V. Dmitryakov, S. N. Chvalun, G. V. Cherkaev, E. A. Svidchenko, T. Ameri, C. J. Brabec, S. A. Ponomarenko, *J. Photonics Energy* **2015**, *5*, 1.
[13] Y.-J. Hwang, F. S. Kim, H. Xin, S. A. Jenekhe, *Macromolecules* **2012**, *45*, 3732.
[14] J. Qi, X. Zhou, D. Yang, W. Qiao, D. Ma, Z. Y. Wang, *Adv. Funct. Mater.* **2014**, *24*, 7605.
[15] V. Cimrová, D. Výprachtický, V. Pokorná, *J. Mater. Chem. C* **2019**, *7*, 8575.
[16] S. Cosnier, A. Karyakin, *Electropolymerization: Concepts, Materials and Applications*, Wiley, Somerset, UK **2011**.
[17] M. D. Imisides, R. John, P. J. Riley, G. G. Wallace, *Electroanalysis* **1991**, *3*, 879.
[18] K. Konkol, R. Schwiderski, S. Rasmussen, *Materials* **2016**, *9*, 404.
[19] R. G. Rajapakse, N. H. Attanayake, D. Karunathilaka, A. E. Steen, N. I. Hammer, D. R. Strongin, D. L. Watkins, *J. Mater. Chem. C* **2019**, *7*, 3168.
[20] S. Li, Y. Ge, S. A. Piletsky, J. Lunec, *Molecularly Imprinted Sensors: Overview and Applications*, Elsevier, Amsterdam **2012**.
[21] Y. Guo, Y. Zhou, *Eur. Polym. J.* **2007**, *43*, 2292.
[22] A. A. Raheem, S. Gopi, M. Kathiresan, C. Praveen, *RSC Adv.* **2019**, *9*, 1895.
[23] A. M. Devasurendra, C. Zhang, J. A. Young, L. V. Tillekeratne, J. L. Anderson, J. R. Kirchhoff, *ACS Appl. Mater. Interfaces* **2017**, *9*, 24955.
[24] M. Bozlar, F. Miomandre, J. Bai, *Carbon* **2009**, *47*, 80.
[25] N. Maráková, Z. A. Boeva, P. Humpolíček, T. Lindfors, J. Pacherník, V. Kašpárková, K. A. Radaszkiewicz, Z. Capáková, A. Minařík, M. Lehocký, *Mater. Sci. Eng. C* **2019**, *105*, 110029.
[26] R. Di Pietro, T. Erdmann, J. H. Carpenter, N. Wang, R. R. Shivhare, P. Formanek, C. Heintze, B. Voit, D. Neher, H. Ade, A. Kiriy, *Chem. Mater.* **2017**, *29*, 10220.
[27] W. Li, K. H. Hendriks, M. M. Wienk, R. A. J. Janssen, *Acc. Chem. Res.* **2016**, *49*, 78.
[28] B. Tieke, A. R. Rabindranath, K. Zhang, Y. Zhu, *Beilstein J. Org. Chem.* **2010**, *6*, 830.
[29] S. P. Ponnappa, S. Arumugam, H. J. Spratt, S. Manzhos, A. P. O'Mullane, G. A. Ayoko, P. Sonar, *J. Mater. Res.* **2017**, *32*, 810.
[30] B. Sari, M. Talu, F. Yildirim, E. K. Balci, *Appl. Surf. Sci.* **2003**, *205*, 27.
[31] N. Maouche, B. Nessark, *Int. J. Electrochem.* **2011**, *2011*, 670513.
[32] D. L. Wakeham, S. W. Donne, W. J. Belcher, P. C. Dastoor, *Synth. Met.* **2008**, *158*, 661.
[33] H. Hosono, H. Kawazoe, *Mater. Sci. Eng. B* **1996**, *41*, 39.
[34] J. Rogalski, J. Rutkowski, *Crystalline materials for optoelectronics. III-Vs Review* **2003**, *16*, 43.
[35] T. H. Le, Y. Kim, H. Yoon, *Polymers* **2017**, *9*.
[36] J. H. L. Ngai, X. Gao, Y. Li, in *Electrochromic Smart Materials: Fabrication and Applications* (Eds: J. W. Xu, M. H. Chua, K. W. Shah), London Royal Society of Chemistry, London **2019**, pp. 103–128.
[37] S. Ming, S. Zhen, K. Lin, L. Zhao, J. Xu, B. Lu, *ACS Appl. Mater. Interfaces* **2015**, *7*, 11089.
[38] H. Gu, S. Ming, K. Lin, S. Chen, X. Liu, B. Lu, J. Xu, *Electrochim. Acta* **2018**, *260*, 772.
[39] A. Durmus, G. E. Gunbas, P. Camurlu, L. Toppare, *Chem. Commun.* **2007**, 3246.
[40] J. L. Bredas, G. B. Street, *Acc. Chem. Res.* **1985**, *18*, 309.
[41] W. S. Huang, A. G. MacDiarmid, *Polymer* **1993**, *34*, 1833.
[42] W. J. Albery, A. R. Mount, in *Electroactive Polymer Electrochemistry: Part 1: Fundamentals* (Ed: M. E. G. Lyons), Springer US, Boston, MA **1994**, pp. 443–483.
[43] W. J. Albery, A. R. Mount, *J. Chem. Soc., Faraday Trans.* **1994**, *90*, 1115.
[44] X. Ren, P. G. Pickup, *Electrochim. Acta* **2001**, *46*, 4177.
[45] X. Ren, P. G. Pickup, *J. Chem. Soc., Faraday Trans.* **1993**, *89*, 321.

 